Effects of Aggregate Structure and Dimension of Carbon Nanotubes on the Mechanical, Electrical and Thermal Properties of Rubber Composites†

SUNG-WOO KIM[*], HO-KYUN JEONG, YONG-GU KANG and MIN-HYEON HAN

NEXEN Tire Corporation R&D Center, Kyungnam 626-230, Republic of Korea

*Corresponding author: Fax: +82 55 3705366; Tel: +82 55 3705344; E-mail: ksw@nexentire.co.kr

A tyre tread compound, showing good performance and high electrical conductivity, was prepared with a high silica loading and a low loading of multi-wall carbon nanotube in order not to sacrifice the original mechanical properties of the rubber compound. We fabricated styrene-butadiene rubber/natural rubber composites containing carbon black as a general filler and two types of multi-wall carbon nanotube with different structure and dimension, entangled carbon nanotube with short length (<10 µm) and parallel-aligned carbon nanotube bundles with a long length (<120 µm) as a specific filler. The incorporation of the aligned multi-wall carbon nanotube into the high silica rubber compound, even at low loading (0.5 phr), improved the static dissipation to a level that could meet the requirements (<10^8 Ω) for tyres without a measurable decrease in the physical and dynamic properties. The abrasion resistance was also enhanced considerably by 15 % or more.

Key Words: Carbon nanotube, Static dissipation, Abrasion resistance.

INTRODUCTION

Since the discovery of carbon nanotube in 1991[1], they have become one of the most active areas in the field of carbon nanotechnology owing their unique mechanical, electrical and thermal properties caused by the high aspect ratio, low diameter and metallic properties[2-5].

Carbon nanotubes are essentially rolled up graphene sheets that are sealed to form hollow tubes. Single-wall carbon nanotubes (SWNT) are cylindrical tubes with a single outer wall with diameters of only 1-2 nm. Multi-wall carbon nanotubes (MWNT) have many layers of graphene wrapped around the core tube.

The use of multi-wall carbon nanotubes is advantageous in nanocomposites because, unlike single-wall carbon nanotube in which two-thirds are semi-conducting and only one-third are conducting, each individual multi-wall carbon nanotubes is conducting because it contains a large number of concentric single-wall carbon nanotubes.

Although the properties of multi-wall carbon nanotubes are excellent, they have not brought any remarkable improvements in the composite properties because of their poor dispersion due to the large surface area and weak interactions with polymer chains that causes large aggregates. As a result, the hysteresis and elongation as well as fatigue properties are decreased significantly[6].
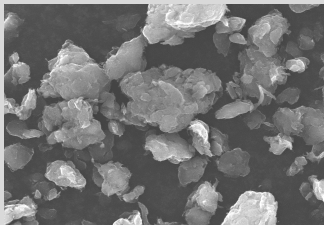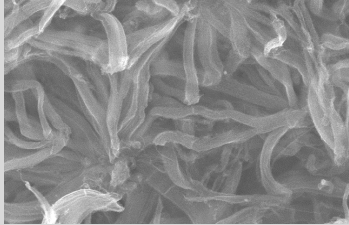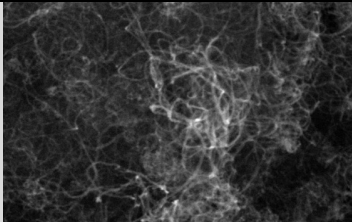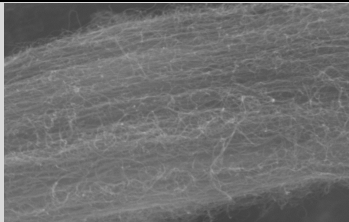
A few technical alternatives can be used to enhance the dispersion of multi-wall carbon nanotubes, such as ultrasonication, ball milling, heat treatment, acid treatment, *in situ* polymerization and latex treatments. On the other hand, it is extremely difficult to produce treated multi-wall carbon nanotubes on a mass production scale. Consequently, the broader use of multi-wall carbon nanotubess is still limited due to the high cost.

Therefore, carbon nanotube has been used mainly in high performance engineering resins and thermoplastics[7-10]. By incorporating carbon nanotubes into commercial high performance plastics and resins, conducting polymers can be prepared for demanding structural and aerospace applications with minimal impact on the mechanical performance. Applications include EMI shielding, static dissipation, electrostatic paint substrates and conductive coupling.

Recently, in the tyre industry, there has been increasing demand for highly silica-filled tyre tread compounds with better rolling resistance and wet grip than conventional carbon black treads due to the more stringent regulations over the world. On the other hand, high loading silica compounds show poor electrical conductivity which is essential for automobile manufacturers to meet the electrical resistance (< 10^8 Ω) for all original equipment tires. A low carbon nanotube loading can be used to impart static dissipation for tread compounds.

†Presented to the International Rubber Conference (IRC-2012), May 21-24, 2012, Jeju, Republic of Korea

TABLE-1 CHARACTERISTICS OF THE E-MWNT AND A-MWNT			
Material		Entangled MWNT	Aligned MWNT
Diameter	Individual CNT (nm)	5~15 nm	5~15 nm
	CNT Bundle (µm)	-	6.5 µm
Length	Individual CNT (µm)	< 10 µm	< 120 µm, Average 80 µm
	CNT Bundle (µm)	-	< 120 µm, Average 80 µm
BET Surface Area (m^2/g)		191	285
Aggregate Structure (SEM x1,000)	Irregular Spherical Type		Long Aligned Type
CNT Bundle Structure (SEM over X5,000)	Random Entangled Type		Parallel Aligned Type

The benefit of such low levels of carbon nanotube addition for static dissipation is that the original mechanical properties of the composites can be maintained.

The types of ingredients and their concentration in rubber compounds affect the mechanical properties. Therefore, the requirements for the materials used in tyre production are quite stringent and qualification is a tedious process. Accordingly, it is advantageous to remain with that formulation once the formulation of a compound is qualified and fixed. Therefore, all mechanical, dynamic and hysteresis properties should be maintained even after adding additional materials, such as carbon nanotube, to the original formulation.

In this study, a tyre tread compound with good performance and high electrical conductivity was prepared using a high volume of silica. The multi-wall carbon nanotubes loading was kept low in order not to sacrifice the original mechanical properties of rubber compound.

Rubber composites with multi-wall carbon nanotube were fabricated and their mechanical, fatigue, electrical, thermal and viscoelastic properties were evaluated. Two types of multi-wall carbon nanotube with different structures and dimensions were used, entangled carbon nanotube with a short length (<10 µm) and vertically aligned carbon nanotube bundles with a long length (<120 µm).

EXPERIMENTAL

The matrix materials were a styrene butadiene rubber with 27 % bound styrene and a 59 % vinyl content in a butadiene unit and natural rubber. The carbon-based nanofillers used were carbon black N339 (OCI Co. Ltd.), entangled multi-wall carbon nanotube (E-MWNT, Carbon Nanotech Co. Ltd.) and aligned multi-wall carbon nanotube (A-MWNT, Hanwha Nanotech Co. Ltd.). Silica (7000 Gr), *bis*-(triethoxysilylpropyl)

tetrasulphide (TESPT), *N*-cyclohexylbenzo thiazole (CBS) and *N,N*'-diphenylguanidine (DPG), zinc oxide (ZnO), stearic acid (S/A), sulfur and processing oil were all supplied by local manufacturers.

Characterization and measurement of properties: Scanning electron microscopy (SEM, JEOL JSM-6490LV) was used to observe the morphology of the pristine carbon nanomaterials. The curing characteristics were measured over a 30-min period at 160 ºC using a Oscillating disk rheometer (ODR) and the tensile properties were measured using a Universal Testing Machine (UTM, Instron Co., UK) at a cross-head speed of 300 mm/min.

The hardness was measured using shore A durometer (TECLOCK) and the fatigue properties of composites using Demattia flex cracking tester (DMFC, UESHIMA). The abrasion weight loss of the rubber composite was investigated using a William type abrasion tester.

The hysteresis properties of the nanocomposites were determined using a Heat Build-Up Flexometer (GABO) for heat generation and dynamic mechanic thermal spectroscopy (DMTS, Eplexor 500 N from GABO) for Tand at 0 ºC and 60 ºC.

The thermal conductivity was characterized using a thermal conductivity analyzer (QTM-500).

The electrical resistance of the rubber composites at room temperature was examined using a two-probe method on a high voltage insulation resistance tester (TERAOHM, MI2077). The two probes measured the electrical resistance at the interface between the probe tip and the nanocomposites.

RESULTS AND DISCUSSION

Table-1 summarizes the characteristics of the two kinds of multi-wall carbon nanotube. One is an entangled multi-wall carbon nanotube (E-MWNT), which has randomly

entangled carbon nanotube chains with a length less than 10 µm and a BET surface area of 191 m²/g. The aggregates had an irregular spherical structure. The other is an aligned multi-wall carbon nanotube (A-MWNT), which has parallel-aligned carbon nanotube chains with lengths up to 120 µm and a BET surface area of 285 m²/g. The aggregates had a well aligned, long bundle structure.

Table-2 summarizes the formulations of the S-SBR/NR composites with multi-wall carbon nanotubes.

TABLE-2
FORMULATIONS OF THE SBR/NR COMPOSITES WITH E-MWNT AND A-MWNT

Material	Compound name (unit : phr)									
	S1	E1	E2	E3	E4	A1	A2	A3	A4	A5
S-SBR	80	80	80	80	80	80	80	80	80	80
NR	20	20	20	20	20	20	20	20	20	20
C/B	20	20	20	20	20	20	20	20	20	20
Silica	40	40	40	40	40	40	40	40	40	40
E-MWNT	-	1	3	5	7	-	-	-	-	-
A-MWNT	-	-	-	-	-	0.5	1	3	5	7
TESPT	3.2	3.2	3.2	3.2	3.2	3.2	3.2	3.2	3.2	3.2
Oil	10	10	10	10	10	10	10	10	10	10

All the composites consisted of solution styrene butadiene rubber and natural rubber as polymer matrices at a ratio of 80:20 and 20 phr of carbon black and 40 phr of silica as the conventional fillers of the tire tread compound. E-MWNT and A-MWNT were used as specific fillers at a ratio of 0.5, 1, 3, 5 and 7 phr.

Table-3 shows the change in Mooney viscosity by the incorporation of multi-wall carbon nanotubes. This dramatic increase was interpreted by the extremely high anisotropy in the shape of the multi-wall carbon nanotube chains and bundles. The A-MWNT composites showed a higher Mooney viscosity than E-MWNT due to the higher aspect ratio of the individual carbon nanotube chains and well aligned long bundle structures of carbon nanotube aggregates of A-MWNT.

Fig. 1 revealed a dramatic increase in modulus at low elongation. This corresponds to the Halpin and Tsai equation

[eqn. (1) - (3)], which is useful for predicting of the composite properties with a non-spherical shape of composite materials and semi-empirical equations developed by curve fitting to consider the aspect ratio of reinforcement and dispersion. When the linear reinforcement of randomly oriented composites is assumed,
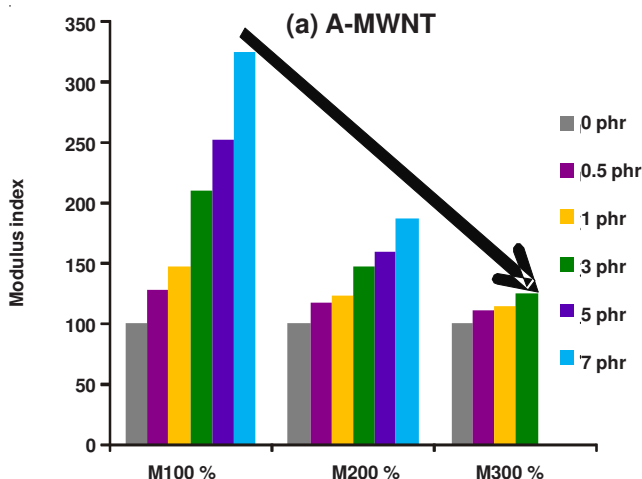
$$E_{para} = E_0(1 + 2f\emptyset)/(1-\emptyset) \qquad (1)$$
$$E_{perp} = E_0(1 + 0.5\emptyset)/(1-\emptyset) \qquad (2)$$
$$E_{rand} = 0.2 \times E_{para} + 0.8 \times E_{perp} \qquad (3)$$

where para, perp and rand stands for parallel, perpendicular and random, respectively, E is the modulus of the composite, E_0 is the modulus of pure composite, f is the aspect ratio of filler and $\emptyset$ is the volume fraction of the filler.

According to Halpin-Tsai theory higher aspect ratio of the filler causes a larger increase in the reinforcement of the modulus. Therefore, high aspect ratio of multi-wall carbon nanotubes can lead to orders of magnitude increases in the stiffening effect compared to spherical particles. The high aspect ratio, anisotropy and alignment of the A-MWNT in the matrix caused a more remarkable increase in the modulus than E-MWNT.

TABLE-3
PHYSICAL, HYSTERETIC, THERMAL AND ELECTRICAL PROPERTIES OF THE NANOCOMPOSITES MIXED WITH E-MWNT AND A-MWNT

|	Compound name									
	S1	E1	E2	E3	E4	A1	A2	A3	A4	A5
Mooney viscosity	69	73	77	83	89	70	74	84	95	105
100 % Modulus (Mpa)	3.1	3.5	4.3	4.6	5.2	4.0	4.6	6.6	7.9	10.2
200 % Modulus (Mpa)	8.7	9.5	11.2	11.6	12.4	10.2	10.8	12.8	13.9	16.3
300 % Modulus (Mpa)	15.0	16.8	17.7	17.9	Failure	16.6	17.2	18.8	Failure	Failure
Hardness	65	67	70	71	73	69	72	75	79	81
Tensile strength (Mpa)	20.0	19.9	19.0	18.4	17.9	18.9	18.9	19.2	18.2	19.0
Elongation (%)	390	340	320	310	280	340	330	310	270	250
HBU (ºC)	22.9	23.5	24.9	27.2	29.3	24.9	25.6	31.3	35.4	35.6
Tan δ at 0 ºC (Wet Grip)	1.122	1.065	0.998	0.983	0.957	1.111	0.960	0.836	0.665	0.591
Tan δ at 60 ºC (rolling resistance)	0.097	0.098	0.101	0.101	0.103	0.098	0.108	0.128	0.151	0.164
Abrasion weight loss (%)	10.08	8.77	7.91	3.72	3.41	8.41	6.26	3.73	1.3	0.68
Crack growth 2,000 cycles (cm)	4.84	5.91	7.35	8.59	9.8	5.34	6.63	10.22	16.42	17.86
Crack growth 6,000 cycles (cm)	8.88	10.16	12.4	13.9	16.94	9.34	10.38	17.68	24.36	Failure
Crack growth 10,000 cycles (cm)	11.4	12.5	15.92	17.84	20.74	12.1	12.9	23.38	Failure	Failure
Thermal conductivity (W/mK)	0.274	0.281	0.289	0.283	0.297	0.279	0.293	0.304	0.321	0.334
Electrical resistivity ($10^8 \Omega$)	231000	224000	1650	5.8	0.4	17.3	0.224	0.033	0.01	0.009
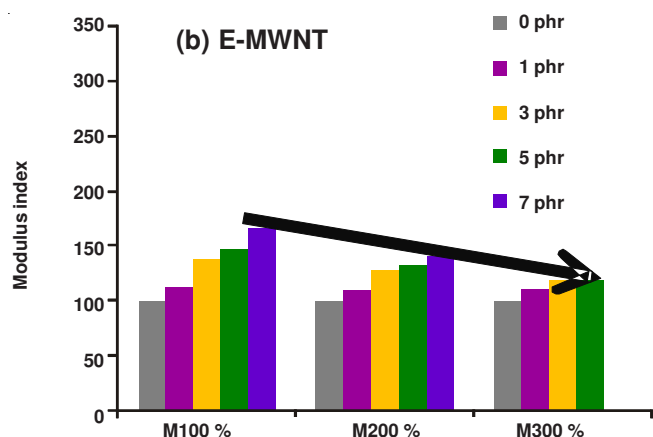
Fig. 1. Modulus index of the nanocomposites with (a) A-MWNT and (b) E-MWNT

The experimentally determined aspect ratio(f) of multi-wall carbon nanotubes in the composites can be predicted using the Halpin-Tsai equation. The theoretical aspect ratio of A-MWNT was approximately 8,000 (L/D = 80 µm/0.01 µm) by the individual A-MWNT chains and approximately 12.3 (L/D = 80 µm/6.5 µm) by the A-MWNT bundles. For the E-MWNT, theoretical aspect ratio was approximately 1,000 (L/D = 10 µm/0.01 µm) by the individual A-MWNT chains. Table- 4 and Fig. 2 present the experimentally determined aspect ratio of the multi-wall carbon nanotubes. E/E_o of the 100 % modulus was calculated using the theoretical aspect ratio as mentioned above. In case of A-MWNT, the predicted E/E_o values calculated using an aspect ratio of 12.3 and 8,000 were significantly different from that calculated from the experimental values. On the other hand, the predicted E/E_o values simulated by using f 250 for A-MWNT and f 70 for E-MWNT corresponded to the experimental E/E_o values. According to the Halpin-Tsai equation the actual diameter and length of the multi-wall carbon nanotube aggregates in the composites were recalculated using f 250 for A-MWNT and f 70 for E-MWNT. The calculated dimensions of the multi-wall carbon nanotubes were 0.32 µm in diameter and 80 µm in length for A-MWNT and 0.14 µm in diameter and 10 µm in length for E-MWNT. This suggests that the multi-wall carbon nanotube are dispersed in the matrix not by individual chains but by divided bundles and aggregate units and also suggests that multi-wall carbon nanotubes in matrix have many curved and linked structures. The predicted E/E_o values at low multi-wall carbon nanotube loadings are slightly lower than the experimental values because the Halpin-Tsai equation was developed for randomly oriented composites, whereas there could be many perfectly aligned structures of multi-wall carbon nanotubes at relatively low concentration.

Table-3 and Fig. 3 show the mechanical and hysteretic properties of the composites. The addition of multi-wall carbon nanotubes caused a dramatic increase in hardness due to the large surface area and high aspect ratio but a significant decrease in elongation, which corresponded to the increased stiffening properties. The multi-wall carbon nanotubes have a negligible effect on the tensile strength.

A-MWNT shows higher heat generation and has adverse effects on the wet grip and rolling resistance compared to E-MWNT because A-MWNT has a strong likelihood of contact and friction under cyclic deformation. The concentration of A-MWNT over 1 phr reduces the elongation and hysteretic properties significantly, whereas a negligible negative effect on those properties is observed at low concentrations of ~0.5 phr or less.

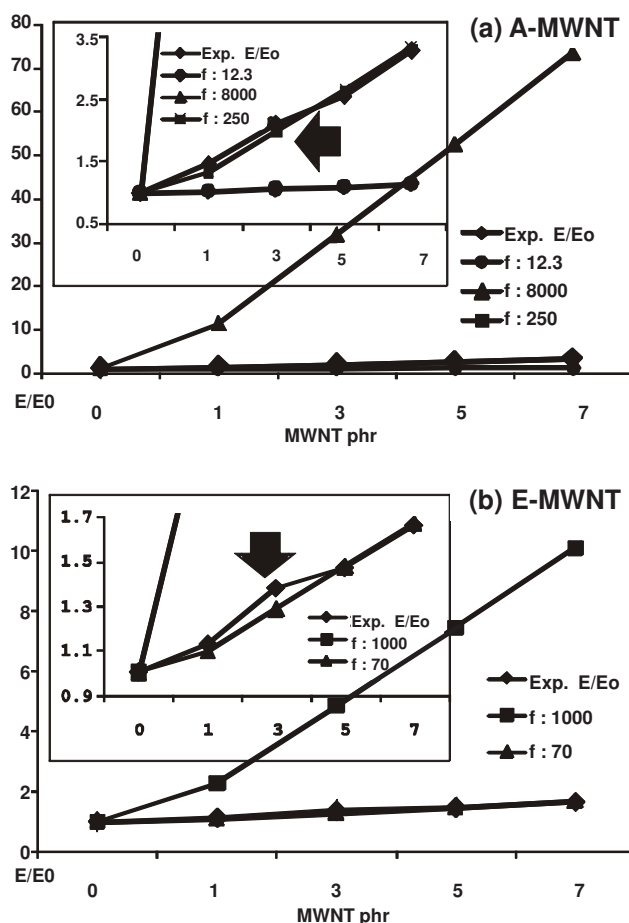| TABLE-4					
EXPERIMENTALLY DETERMINED ASPECT RATIOS OF (a) A-MWNT AND (b) E-MWNT					
(a)	A-MWNT content (phr)	0	1	3	5	7
E/E_o (M-100)	**Experimental Value**	**1**	**1.47**	**2.09**	**2.53**	**3.25**
	Predicted value f : 12.3	1	1.02	1.06	1.10	1.14
	f : 8000	1	11.17	31.71	52.51	73.59
	f : 250	**1**	**1.32**	**1.97**	**2.63**	**3.29**
(b)	E-MWNT Content (phr)	0	1	3	5	7
E/E_o (M-100)	**Experimental Value**	**1**	**1.13**	**1.38**	**1.47**	**1.66**
	Predicted value f : 1000	1	2.28	4.85	7.46	10.10
	f : 70	**1**	**1.09**	**1.28**	**1.47**	**1.67**

Fig. 2. Experimentally determined aspect ratios of (a) A-MWNT and (b) E-MWNT

Table-3 and Fig. 4 present the abrasion and fatigue properties. By incorporating A-MWNT into the rubber composites, the abrasion property increased dramatically whereas the fatigue property decreased exponentially. Even a 0.5 phr loading of A-MWNT produced a 17 % increase in abrasion resistance with almost no adverse effect on crack growth.

Fig. 5 shows that the thermal and electrical conductivity of the A-MWNT composites were enhanced remarkably compared to the E-MWNT composites and the composite
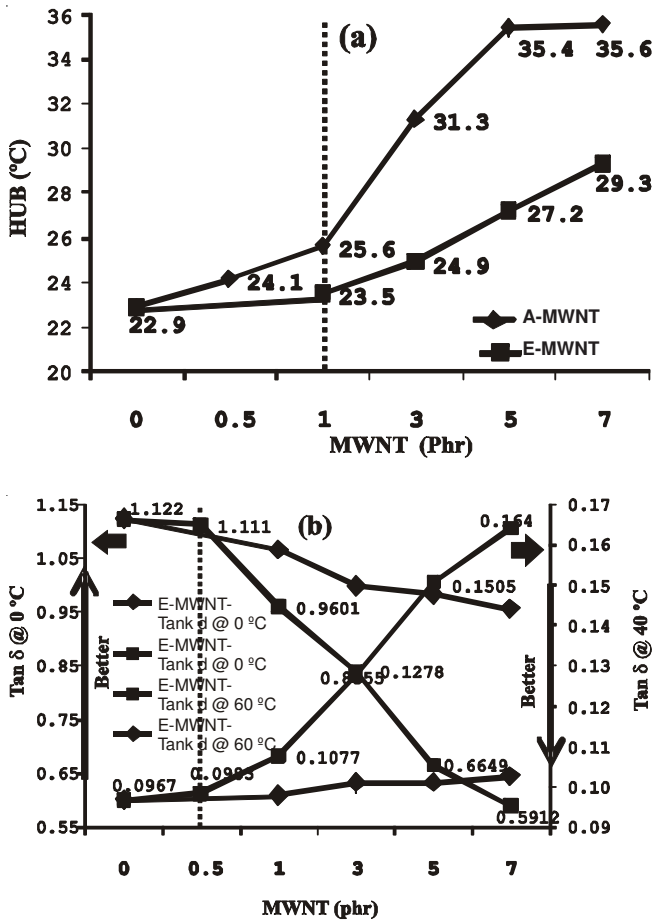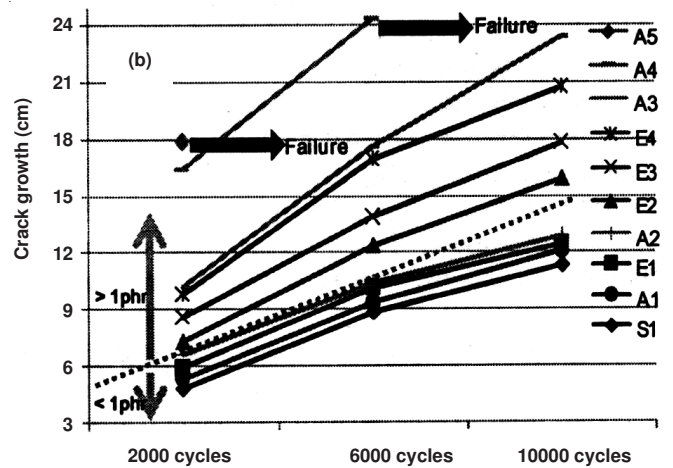
Fig. 4.   Abrasion and fatigue properties of the MWNT nanocomposites; (a) abrasion index and (b) crack growth

Fig. 3.   Hysteresis properties of the MWNT nanocomposites ; (a) HBU and (b) Tan δ at 0 ℃ and 60 ℃

without MWNTs due to high anisotropy and well aligned long bundle structures of A-MWNT aggregates, which make it easy to abut or contact each other to form a conducting network. At a critical volume fraction (the percolation threshold), conducting paths and interconnecting filler networks form leading to a sharp decrease in the electrical resistance. Interconnecting filler networks are not formed below the critical volume fraction of carbon nanomaterials, which result in a large increase in the electrical resistance of the nanocomposites. The percolation threshold was 0.5 phr for A-MWNT and 5 phr for E-MWNT,
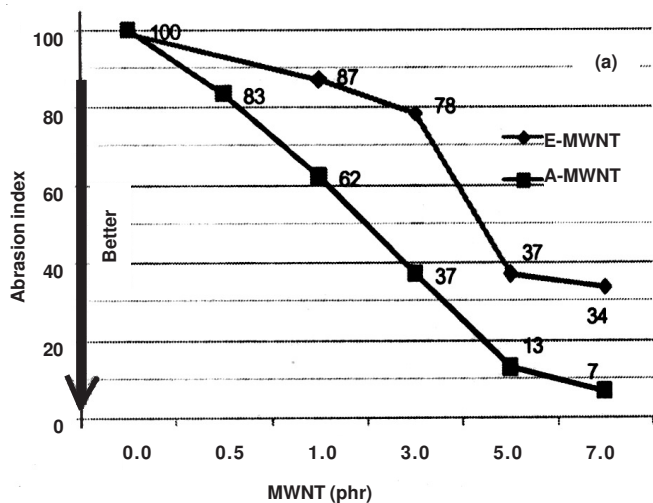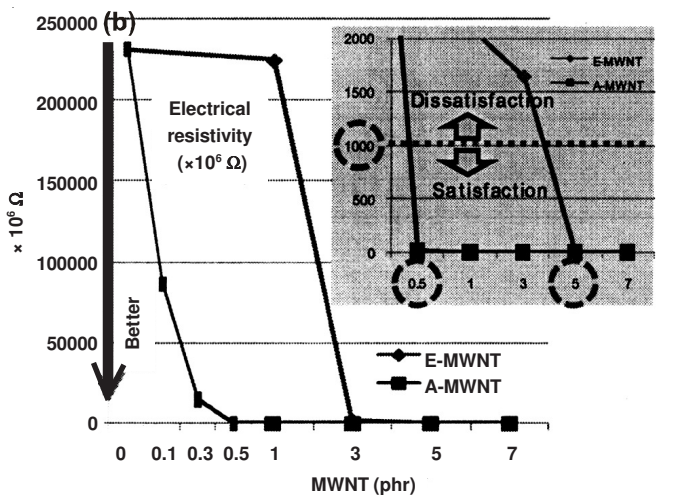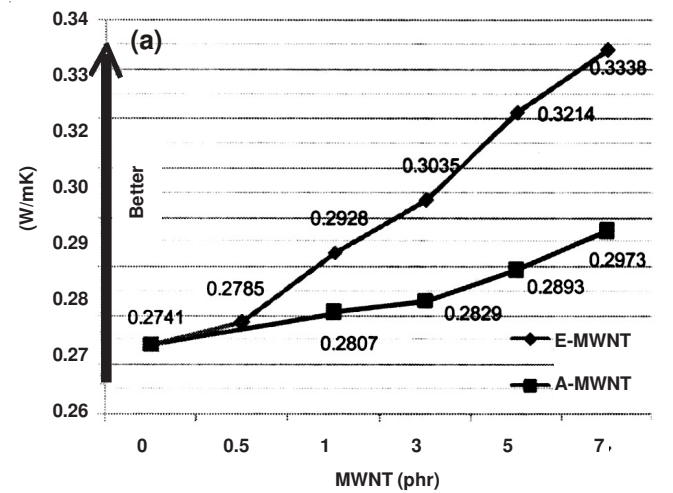

Fig. 5.   Thermal and electrical properties of the MWNT nanocomposites ; (a) thermal conductivity and (b) electrical resistivity

as shown in Fig. 5. In other words, even at a low A-MWNT loading of 0.5 phr, A-MWNT enabled high silica rubber composites to obtain satisfactory static dissipation properties to the level that could meet the requirements of below 10^8 Ω, whereas E-MWNT showed dissatisfactory electrical conductivity up to 5 phr due to structural disadvantages such as short

length, entangled carbon nanotube chains and irregular spherical types of E-MWNT aggregates.

Conclusion

Styrene-butadiene rubber/natural rubber composites, which contain carbon black as a general filler and multi-wall carbon nanotube as specific fillers, were fabricated and their mechanical, fatigue, electrical, thermal and viscoelastic properties were evaluated.

A viable solution was developed for applications of tire tread compounds with high silica loadings that require high conductivity combined with good mechanical properties.

The extremely low loadings(~0.5 phr) of long aligned multi-wall carbon nanotube, which has a long length (<120 μm) and aligned bundle structures of their aggregates, can also meet the static dissipation requirements with no measurable adverse change in the original tread compound properties, such as tensile, fatigue, heat generation, wet grip and rolling resistance. Moreover, the abrasion resistance was enhanced considerably by more than 15 %.

REFERENCES

1. S. Iijima, *Nature*, **354**, 56 (1991).
2. O. Chauvet, J.M. Benoit and B. Corraze, *Carbon*, **42**, 949 (2004).
3. J.Z. Liu, Q.S. Zheng, L.F. Wang and Q. Jiang, *J. Mech. Phys. Solids*, **53**, 123 (2005).
4. C.Q. Sun, H.L. Bai, B.K. Tay and E.Y. Jiang, *J. Phys. Chem. B*, **107**, 7544 (2003).
5. N. Mingo and D.A. Broido, *Nano Lett.*, **5**, 1221 (2005).
6. F. Cataldo, O. Ursini and G. Angelini, *Fullerenes, Nanotubes Carbon Nanostructures*, **17**, 38 (2009).
7. M.S.P. Shaffer, X. Fan and A.H. Windle, *Carbon*, **36**, 1603 (1998).
8. L. Cai, J.L. Bahr, Y. Yao and J.M. Tour, *Chem. Mater.*, **14**, 4235 (2002).
9. E.T. Mickelson, C.B. Huffman, A.G. Rinzler, R.E. Smalley, R.H. Hauge and J.L. Margrave, *Chem. Phys. Lett.*, **296**, 188 (1998).
10. J.L. Bahr, J. Yang, D.V. Kosynkin, M.J. Bronikowski, R.E. Smalley and J.M. Tour, *J. Am. Chem. Soc.*, **123**, 6536 (2001).